

$$\begin{aligned} \Delta E_m &= \frac{1}{2} M_m x_i^2 \\ &= \frac{1}{2} M_m \left\{ \sum_{k=1}^{2n} [u_{ik} v_k x(0)]^2 e^{2\lambda_k t} \right. \\ &\quad \left. + \sum_{k=1}^{2n-1} \sum_{r=k+1}^{2n} 2[u_{ik} u_{ir}][v_k x(0)][v_r x(0)] e^{(\lambda_k + \lambda_r) t} \right\} \end{aligned} \quad (5)$$

(m=1,2,...,n, i = m + n)

where M_m is the inertia constant.

Comparison of Eq. (4) and Eq. (5) indicates that there are many more "energy modes" than "motion modes". In addition, we note that, because each energy mode is a combination of 2 motion modes, energy modes will have damping factors and frequencies different from those of any motion mode.

Suppose there are 4 motion modes in Eq. (4). They are listed in Table 1.

Table 1 The motion modes of a system

Mode number	mode	Angular speed (rad/sec)
1	$\alpha_1 + j\beta_1$	β_1
2	$\alpha_1 - j\beta_1$	β_1
3	$\alpha_2 + j\beta_2$	β_2
4	$\alpha_2 - j\beta_2$	β_2

The energy modes, listed in Table 2, are the combinations of motion modes.

Table 2 The energy modes of a system

mode number	combination of motion modes	energy mode	Angular speed (rad/sec)
A	1-1	$2\alpha_1 + j2\beta_1$	$2\beta_1$
B	2-2	$2\alpha_1 - j2\beta_1$	$2\beta_1$
C	3-3	$2\alpha_2 + j2\beta_2$	$2\beta_2$
D	4-4	$2\alpha_2 - j2\beta_2$	$2\beta_2$
E	1-3	$\alpha_1 + \alpha_2 + j(\beta_1 + \beta_2)$	$\beta_1 + \beta_2$
F	2-4	$\alpha_1 + \alpha_2 - j(\beta_1 + \beta_2)$	$\beta_1 + \beta_2$
G	1-4	$\alpha_1 + \alpha_2 + j(\beta_1 - \beta_2)$	$\beta_1 - \beta_2$
H	2-3	$\alpha_1 + \alpha_2 - j(\beta_1 - \beta_2)$	$\beta_1 - \beta_2$
I	1-2	$2\alpha_1$	0
J	3-4	$2\alpha_2$	0

It is noted that mode A - mode B, mode C - mode D, mode E - mode F, and mode G - mode H are conjugate modes respectively. The frequencies of mode I and mode J are zero.

II. 3 ENERGY INTERCHANGE IN A TWO-MACHINE SYSTEM

To make subsection II. 4 easily understood, let us consider a two-machine system shown schematically in Figure 1.

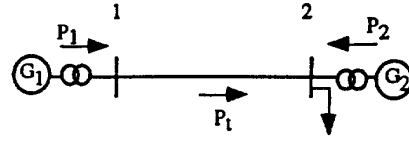


Fig. 1 A two-machine system

In Figure 1, P_1 , P_2 , and P_t are the real powers of generators 1, 2, and tie-line, respectively. Let $\theta_{12} = \theta_1 - \theta_2$ and $\omega_{12} = \omega_1 - \omega_2$ be the relative rotor angle and the relative rotor speed of generator 1 respectively.

II. 3.1 Energy Interchange and Choice of Coordinate System

The generators are modeled classically without damping and the equations of motion for this system are

$$\begin{cases} \dot{\theta}_i = \omega_i - \omega_s \\ M_i \dot{\omega}_i = P_{mi} - P_i \end{cases} \quad (6)$$

where ω_s is the synchronous speed and P_{mi} the mechanical input. (Throughout subsection II. 3, $i = 1, 2, n=2$.)

Let $M_T = \sum_{j=1}^n M_j$ and define the Center of Inertia (COI) for the system as

$$\begin{cases} \Theta_0 = (\sum_{j=1}^n M_j \theta_j) / M_T \\ \Omega_0 = (\sum_{j=1}^n M_j \omega_j) / M_T \end{cases} \quad (7)$$

We transform the variables θ_i , ω_i to the COI variables as $\Theta_i = \theta_i - \Theta_0$, $\Omega_i = \omega_i - \Omega_0$. Eq. (6) becomes [8,p. 27]

$$\begin{cases} \dot{\Theta}_i = \Omega_i \\ M_i \dot{\Omega}_i = f_i(\Theta) \end{cases} \quad (8)$$

for $f_i(\Theta)$, see [8].

We note that in COI

$$\begin{cases} \Omega_1 = M_2(\omega_1 - \omega_2) / M_T \\ \Omega_2 = -M_1(\omega_1 - \omega_2) / M_T \end{cases} \quad (9)$$

Suppose the stable equilibrium point of the post-fault system is $\Theta_i = \Theta_i^s$, $\Omega_i = 0$, the individual machine energy function is [8,p. 28-30]

$$\begin{aligned} V_i(\Theta, \Omega) &= M_i \Omega_i^2 / 2 - \int_{\Theta_i^s}^{\Theta_i} f_i(\Theta) d\Theta_i \\ &= V_{KEi} + V_{PEi} \end{aligned} \quad (10)$$

where

$$V_{KEi} = M_i \Omega_i^2 / 2 \quad (11.1)$$

$$V_{PEi} = - \int_{\Theta_i}^{\Theta_i} f_i(\Theta) d\Theta_i \quad (11.2)$$

V_{KEi} is the kinetic energy and V_{PEi} is the potential energy.

Based on Eqs.(9), we note that, in COI, generators 1 and 2 always swing against each other, but based on Eq. (11.1), we can not observe energy exchange simply by inspecting kinetic energy because all V_{KEi} are in phase.

We investigate the energy interchange in the system by applying a three-phase fault at Bus 1, cleared at 0.05 seconds. The dynamic behaviors of two machines are obtained from time domain simulation.

In Figures 2-4, KE is the kinetic energy (in pu), and PE is the potential energy (in pu), calculated based on Eqs. (11.1) and (11.2), and the numbers 1 and 2 stand for generators 1 and 2, respectively.

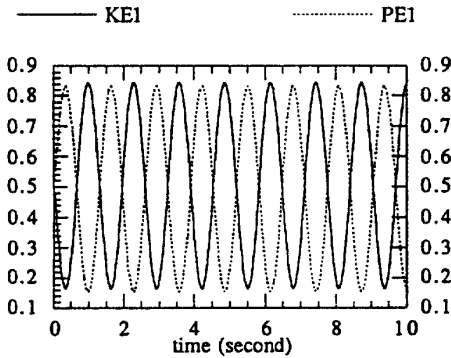


Fig. 2 Energy interchange of generator 1 in COI

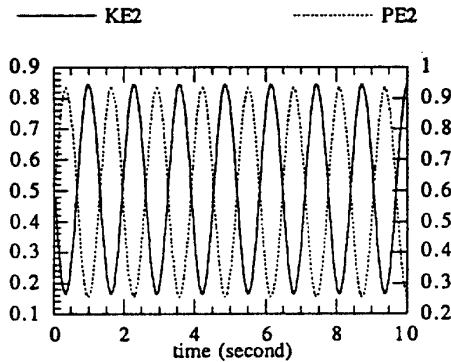


Fig. 3 Energy interchange of generator 2 in COI

It is noted from Figures 2 and 3 the antiphase behavior between kinetic energy and potential energy. Therefore, the kinetic energy interchanges with the potential energy for each machine.

The energy interchange is also investigated through the kinetic energy alone in Synchronous Coordinate Framework

(SCF). Figure 5 shows the kinetic energies (in pu) of generators 1 and 2, calculated based on Eq. (5).

We note from Figure 4 that energy interchange can be observed via the antiphase behavior of the kinetic energy in SCF.

The above discussion indicates that a proper coordinate framework is necessary for analysis of energy interchange, and that we can identify generators exchanging energy during SIAO using phase of kinetic energy expression in SCF.

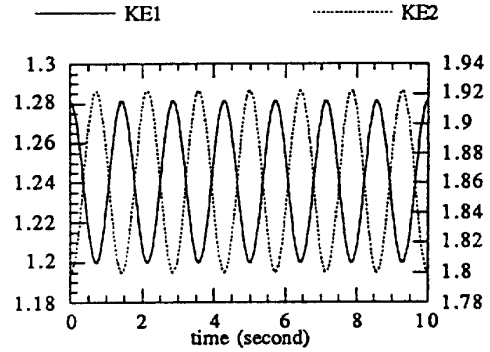


Fig. 4 Energy interchange in SCF

Now let us discuss the kinetic energy interchange in SCF in detail.

II. 3.2 Energy Interchange in SCF

Linearizing Eq. (6), we get

$$\begin{cases} \Delta \dot{\theta}_i = \Delta \omega_i \\ \Delta \dot{\omega}_i = -K_i \Delta \theta_{12} / M_i \end{cases} \quad (13)$$

where

$$K_i = \left. \frac{\partial P_i}{\partial \theta_{12}} \right|_{\theta_{12} = \theta_{120}}$$

θ_{120} - the post-disturbance stable equilibrium point.

$$\text{Let } a = -K_1 / M_1 + K_2 / M_2 \quad (14)$$

[9] The system is stable if $a < 0$. The motion modes of this system are $\omega = \pm j\sqrt{-a}$ and its solution is

$$\begin{aligned} \Delta \omega_i &= -\frac{2K_i C}{\omega M_i} \sin(\omega t + \varphi) + \Delta \omega_i(t_{cl}) + \frac{2K_i C}{\omega M_i} \sin(\omega t_{cl} + \varphi) \\ &\equiv \xi_i \sin(\omega t + \varphi) + \eta_i \\ &\equiv |\xi_i| \sin(\omega t + \varphi + \phi_{\omega i}) + \eta_i \end{aligned} \quad (15)$$

where

$$\begin{aligned} C &= |\omega \Delta \theta_{12}(t_{cl}) - j \Delta \omega_{12}(t_{cl})| / 2\omega \\ \varphi &= \tan^{-1}(-\Delta \theta_{12}(t_{cl}) / \omega \Delta \omega_{12}(t_{cl})) \\ \phi_{\omega i} &= \cos^{-1}(\xi_i / |\xi_i|) \end{aligned}$$

The subscript cl is used to indicate the values at clearing time. $C > 0$. The ϕ_{ω} , named the phase of the coefficient of motion mode, yields the same information as mode shape from eigenanalysis.

It is noted from Eq. (15) that generators 1 and 2 swing against each other under the condition:

$$\phi_{\omega 1} - \phi_{\omega 2} = \pm 180^\circ \quad (16.1)$$

i.e.,

$$K_1 K_2 < 0 \quad (16.2)$$

The kinetic energy deviation of generator i is

$$\begin{aligned} \Delta E_i &= \frac{1}{2} M_i \left\{ \xi_i^2 \sin^2(\omega x + \varphi) + 2 \xi_i \eta_i \sin(\omega x + \varphi) + \eta_i^2 \right\} \\ &= \frac{1}{2} M_i \left\{ \xi_i^2 \sin^2(\omega x + \varphi) + 2 |\xi_i \eta_i| |\sin(\omega x + \varphi + \phi_{Ei})| + \eta_i^2 \right\} \end{aligned} \quad (17)$$

where

$$\begin{aligned} \sin^2(\omega x + \varphi) &= (1 - \cos(2\omega x + 2\varphi)) / 2 \\ \phi_{Ei} &= \cos^{-1}(\xi_i \eta_i / |\xi_i \eta_i|) \end{aligned}$$

The energy modes are $\pm j\omega$ and $\pm j2\omega$. The ϕ_{Ei} is named the phase of the coefficient of energy mode. Because the first and third terms in Eq. (17), corresponding to the motions of rotor, are always greater than zero, it is impossible for them to represent energy interchange.

Only the second term in Eq. (17) can represent energy interchange under the condition:

$$\phi_{E1} - \phi_{E2} = \pm 180^\circ \quad (18.1)$$

$$\text{i.e., } (\xi_1 \eta_1)(\xi_2 \eta_2) < 0 \quad (18.2)$$

The analytical results from a two-machine system, specifically Eqs. (16.1), (16.2), (18.1), and (18.2) in SCF, and also Eqs. (9) and (11.1) in COI, indicate that the swing pattern may be obtained by comparing for all machines the phase of the coefficient of motion modes, and that the energy interchange pattern may be obtained by comparing for all machines the phase of the coefficient of energy modes in kinetic energy expression in SCF. We note that there is no reason to expect the two patterns will be the same.

II. 4 ENERGY INTERCHANGE AND PHASE OF ENERGY MODES

Now we extend the result in last subsection to a system with n classical generators, in which there are 2n motion modes. The number of energy modes is given by Eq. (19). There may be some energy modes whose values are zero because of the zero eigenvalues or conjugate eigenvalues in the motion modes.

$$N = n(1 + 2n) \quad (19)$$

Table 2 suggests that a general form for Eq. (5) is:

$$\Delta E_m = \sum_{k=1}^N a_{mk} e^{\lambda_k t} \quad (20)$$

The physical meaning of the phase of the coefficient of kinetic energy for a pair of conjugate modes is discussed as follows:

Consider a pair of conjugate energy modes in Eq. (20) $\lambda_p = \sigma_p + j\omega_p$ and $\lambda_{p+1} = \sigma_p - j\omega_p$ which arise as a combination of a pair of motion modes.

The terms which are corresponding to these two modes in Eq.(20) are given by Eq.(21)

$$\Delta E_{mp} = a_{mp} e^{\lambda_p t} + a_{mp+1} e^{\lambda_{p+1} t} \quad (21)$$

where

$$\begin{aligned} a_{mp} &= A_{mp} (\cos \phi_{mp} + j \sin \phi_{mp}) \\ a_{mp+1} &= A_{mp} (\cos \phi_{mp} - j \sin \phi_{mp}) \end{aligned} \quad (22)$$

Therefore, Eq. (21) can be rewritten as

$$\Delta E_{mp} = 2A_{mp} e^{\sigma_p t} \cos(\omega_p t + \phi_{mp}) \quad (23)$$

Let ϕ_{ip} be the phase of the coefficient of kinetic energy deviation corresponding to generator i for modes p and p+1, and ϕ_{jp} be that corresponding to generator j for the same conjugate modes p and p+1.

If $\phi_{ip} - \phi_{jp} = \pm 180^\circ$ then the modes p and p+1 interchange energy between generator i and generator j. The energy interchange of modes p and p+1 may involve more than two generators in the system.

Since there are many energy modes, we will obtain information regarding the energy interchange pattern by identifying all machines in the system whose kinetic energy deviation has a relatively high coefficient, in magnitude, for the same energy mode. Inspection of the phase of the coefficient for each generator relative to each other indicates whether they are involved in an energy interchange.

The kinetic energy deviation for generator i is

$$\Delta E_m = \sum_{j=1}^{N_2} 2A_{mj} e^{\sigma_j t} \cos(\omega_j t + \phi_{mj}) \quad (24)$$

If all eigenvalues of the system are complex, we have

$$N_2 = N / 2 \quad (25)$$

Suppose that we use the first N_3 biggest terms to approximate Eq. (24), we rewrite Eq. (24) in a descending order in terms of the coefficients as follows

$$\Delta E_m \approx \sum_{j=1}^{N_3} 2A_{mj} e^{\sigma_j t} \cos(\omega_j t + \phi_{mj}) \quad (26)$$

where

$$N_3 \ll N_2 \quad (27)$$

We will inspect the phase (ϕ_{mj} in Eq. (26), $m = 1, 2, \dots, n$) of the coefficient of the lightly damped or undamped energy modes named dominant interarea energy modes (DIEMs), which are a combination of two interarea modes, i.e., they will appear in Eq. (2) for several generators.

For a system there may be several DIEMs, each of which have a distinct energy interchange pattern.

III. NUMERICAL RESULT

The procedures developed in sections II are tested in the equivalent 19-generator WSCC system. Figure 5 shows its one line diagram.

The 19-generator system has 38 oscillation modes in the low frequency range (0.1-3.0 Hz), which are listed in Table 3. In Table 3, Re. and Im. stand for real and imaginary respectively. The mode numbers with an asterisk are interarea modes and the others are local modes. Participating generators in each mode are determined using participation factors.

Mode shapes of rotor speeds have been widely used for identification of the oscillation pattern of a particular mode. The phase of right eigenvectors of rotor speed can be used to group areas which swing in the same direction. The phase of right eigenvectors of five interarea modes are listed in Table 4.

It is noted from Table 4 that, in each mode, the areas in the system can be grouped into two which swing against each other. For mode 24 (0.7 Hz), generators 1, 4, 5, 14, 15, 16, 17, 18, and 19 swing against another group consisting of generators 2, 3, 7, 8, 9, 10, 11, and 12. Generators 6 and 13 are not involved in this mode because their participation factors related to this mode are zero.

We apply the proposed method of analyzing the energy interchange by applying a three-phase fault at Bus 26, cleared at 0.05 seconds. To verify results, the dynamic behaviors of the rotor speeds of 19 machines are obtained from time domain simulation, in which a fully nonlinear model of the system is employed.

For the 19-machine system, there are 38 motion modes so that there are $(1+38)19 = 741$ energy modes. The coefficients for each energy mode of the kinetic energy deviation of each machine is calculated based on Eq. (24). Here we choose the first 40 ($N_3 = 40$) largest coefficients for each machine. We can obtain the energy interchange pattern by (a) identifying all machines in the system whose kinetic energy deviation has a relatively high coefficient in magnitude for the same energy mode, and (b) inspecting the phase of the coefficient for each machine relative to each other.

Since the energy mode which is the combination of interarea modes 14 and 24 satisfies the dominate energy mode condition as discussed in section II, the energy interchange pattern of this energy mode is analyzed by comparing the phase of coefficient of the kinetic energy deviation of each generator for this dominant energy mode. The result is shown in Table 5 where X means the coefficient of the energy mode corresponding to this generator is very small.

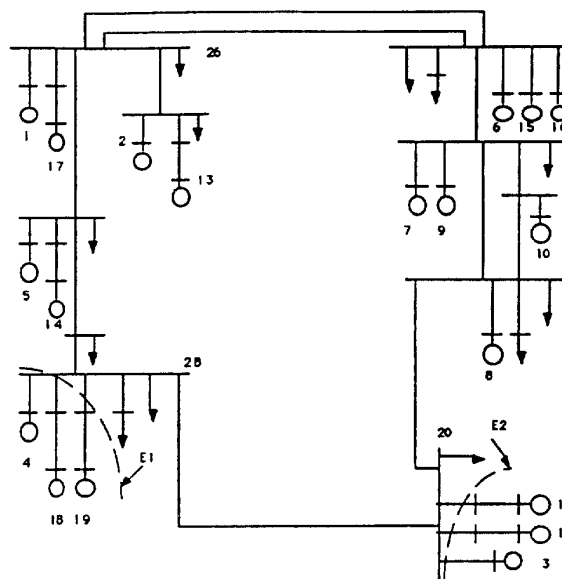


Fig. 5 The one line diagram of the testing system

Table 3 The eigenanalysis result

Mode	Re. Part	Im. Part	Frequency (Hz)	Participating Generators
2	-0.05	11.51	1.83	15
4	-0.04	10.95	1.74	13
6	-0.06	9.42	1.51	14
8	-0.03	8.67	1.38	18
10	-0.05	10.81	1.72	17
*12	-0.008	5.95	0.95	4,5,6,9,14,18
*14	-0.007	2.04	0.33	2,3,4,6,11
16	-0.07	12.73	2.03	1
18	-0.06	10.24	1.63	19
20	-0.04	7.11	1.13	9
22	-0.06	11.87	1.89	11
*24	-0.0066	4.41	0.70	2,3,4,5,8,10,11,14,18,19
*26	-0.009	4.07	0.65	2,6,8,10,13
*28	-0.01	5.08	0.81	2,3,4,6,8,9,10,18,19
31	-0.08	14.51	2.32	12
33	-0.08	13.97	2.24	16
35	-0.09	13.21	2.20	10
37	-0.09	14.75	2.35	7

It is found from Table 5 that the machines can be divided into two groups that interchange energy with each other in terms of this energy mode. For the energy mode which consists of the combination of motion modes 14 and 24, group 1 consisting of generators 2, 4, 8, 10, 13, 18, and 19 interchanges energy with group 2 consisting of generators 3, 5, 11, and 12.

Of generators in group 1, generators 4, 10, 18, and 19 have magnitudes larger than $1.5 \cdot 10^{-3}$. We note from Figure 5 that

generators 4, 18, and 19 are tightly couple and in the same geographic area, denoted by E1. Of generators in group 2, generators 3, 11, and 12 have magnitudes larger than $1.5 \cdot 10^{-3}$. We note from Figure 5 that these generators are also tightly coupled and in the same geographic area, denoted by E2. Areas E1 and E2 are connected through tie-line 28-20. It is likely that this tie-line would be an effective location for installing a FACTS-type controller. We are presently investigating this possibility.

Table 4 The phase of right eigenvectors (degrees)

Generator	Mode 12	Mode 14	Mode 24	Mode 26	Mode 28
1	90	-92	90	-90	90
2	-90	-95	-93	95	-90
3	-90	88	-90	90	90
4	90	83	90	90	-94
5	-90	-90	86	75	-90
6	90	-93	76	-90	90
7	90	-95	-83	-90	87
8	-90	-104	-90	-96	-90
9	90	-96	-95	-90	82
10	-90	-110	-90	-93	-90
11	-90	83	-90	90	90
12	-90	81	-90	90	90
13	-90	-93	-95	-92	-90
14	-90	-90	84	-75	-103
15	90	-97	79	-90	90
16	90	-91	81	-90	90
17	90	-93	90	-90	90
18	90	86	90	90	-98
19	90	82	90	90	-99

In Figures 6 and 7, KE3, KE4, and KE10 represent the kinetic energies (in pu) of generators 3, 4, and 10, respectively.

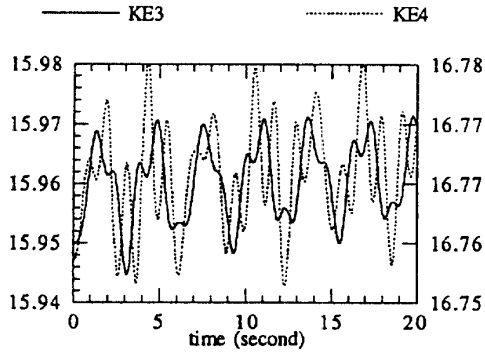


Fig. 6 Energy interchange between generators 3 and 4

Figure 6 shows the kinetic energies of generators 3 and 4. The antiphase behavior of the two plots verifies the predicted energy interchange pattern.

Figure 7 shows the kinetic energies of generators 3 and 10. It is noted from Figure 5 that generators 3 and 10 are far away from each other. The energy interchange between generators

3 and 4, physically located far from each other, is also verified by the antiphase behavior of the two plots.

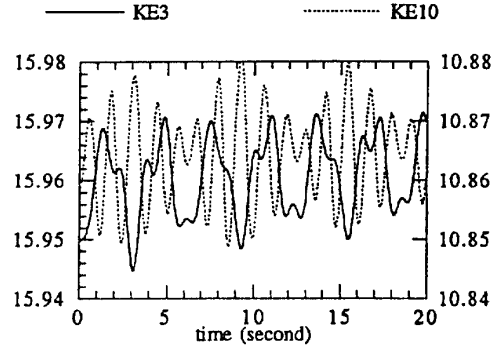


Figure 7 Energy interchange between generators 3 and 10

Table 5 The energy interchange pattern

Generator	mode 14-24	
	Magnitude $\times 10^{-3}$	Phase (degree)
1	X	
2	1.08	177.8
3	2.27	-1.35
4	3.67	178.7
5	0.73	-1.42
6	X	
7	X	
8	1.17	178.5
9	X	
10	2.16	178.5
11	1.59	-1.36
12	1.64	-1.36
13	1.42	177.8
14	X	
15	X	
16	X	
17	X	
18	2.203	178.7
19	2.04	178.7

A summary comparing the results from eigenanalysis and the those from the proposed energy method is given in Table 6 where GEN stands for generator and DIEM stands for Dominant Interarea Energy Modes. This table points out that mode shape, as derived from eigenanalysis, does not necessarily reflect the energy interchange pattern. For example, mode shape indicates that generators 3 and 5 swing against each other in both modes 14 and 24. However, energy analysis indicates that these two generators do not interchange energy. Table 6 indicates other generators for which mode shape does not reflect the energy interchange pattern. Table 6 also indicates that the results obtained from the proposed method agree well with those obtained from time simulation. Therefore, the proposed method is effective in identifying the energy interchange pattern whereas mode shape may be misleading if interpreted as providing information about energy interchange.

Table 6 The comparison of the numerical results

From Table 4 (mode shape)	From Table 5 (proposed method)	From Figs. 5 and 6 (time simulation)
<p><u>Interarea mode 14:</u></p> <p>GENs 3 and 4 swing together.</p> <p>GEN 3 swings against GEN 10.</p> <p>GEN 3 swings against GEN 5.</p> <p><u>Interarea mode 24:</u></p> <p>GEN 3 swings against GEN 4.</p> <p>GENs 3 and 10 swing together.</p> <p>GEN 3 swings against GEN 5.</p>	<p><u>DIEM 14-24:</u></p> <p>GENs 3 and 4 interchange energy each other.</p> <p>GENs 3 and 10 interchange energy each other.</p> <p>GENs 3 and 5 are in the same group.</p>	<p><u>DIEM 14-24:</u></p> <p>GENs 3 and 4 interchange energy each other.</p> <p>GENs 3 and 10 interchange energy each other.</p> <p>GENs 3 and 5 are in the same group (figure not shown).</p>

IV. CONCLUSIONS

An energy approach to analysis of SIAO in power systems has been developed. A proper coordinate framework is necessary for analysis of energy interchange. We can identify generators exchanging energy during SIAO using phase of kinetic energy expression in synchronous coordinate framework. It is confirmed, from both analytical method and numerical result, that SIAO is characterized as oscillatory behavior, following a disturbance, of the rotor motion with respect to a synchronous reference frame, for two or more generator groups such that there is a periodic interchange of energy between them. It can be seen through the numerical result of the equivalent WSCC system that this approach gives an improved understanding of the fundamental nature of SIAO. This information may be useful in locating effective controllers.

V. ACKNOWLEDGMENT

This work was funded in part by the National Science Foundation under grant ECS-9309092, and in part by the Electric Power Research Center of Iowa State University, to whom grateful acknowledgment is due.

VI. REFERENCES

1. de Mello, F.P., et. al., "Concepts of synchronous machine stability as affected by excitation control", IEEE Trans. on Power Apparatus and Systems, Vol. PAS-88, pp. 316-329, April, 1969
2. Perez-Arriaga, I., et. al., "Selective modal analysis with application to electric power systems", IEEE Trans. on

Power Apparatus and Systems, Vol. PAS - 101, No. 9, pp. 3117-3134, Sept. 1982

3. Mansour, Y., "Application of eigenanalysis to the Western North American Power System", IEEE 90TH0292-3-PWR, pp. 97-104
4. Klein, M., et. al., "A fundamental study of inter-area oscillations in power systems", IEEE/PES Winter Meeting, New York, New York, Feb. 3-7, 1991.
5. Ostojic, D.R., "Spectral monitoring of power system dynamic performances", IEEE Trans. on Power System, Vol. 8, No. 2, pp. 445-451, May 1993
6. Anderson, P.M., Fouad, A.A., Power System Control and Stability, Vol. 1, Ames, Iowa, The Iowa State University Press, 1977
7. Ilic, M., et. al., "A simple structure approach to modeling and analysis of the interarea dynamics of the large electric power systems: Part I - linearized models of frequency dynamics", Proceeding of 1993 Northern American Power Symposium, Washington DC, Oct. 1992
8. Pai, M.A., Energy Function Analysis for Power System Stability, Norwell, Massachusetts, Kluwer Academic Publishers, 1989.
9. Venikov, V. "Transient processes in electrical power systems," MIR publishers, Moscow, 1977, pp 335-337.